Research Article | Vol. 12, No. 2 / 1 February 2021 / Biomedical Optics Express 756
Biomedical Optics EXPRESS

Assessment of the corneal collagen organization after chemical burn using second harmonic generation microscopy

JUAN M. BUENO,[1,*] FRANCISCO J. ÁVILA,[2] ELVIRA LORENZO-MARTÍN,[3] PATRICIA GALLEGO-MUÑOZ,[3] AND M. CARMEN MARTÍNEZ-GARCÍA[3]

[1]*Laboratorio de Óptica, Instituto Universitario de Investigación en Óptica y Nanofísica, Universidad de Murcia, Campus de Espinardo (Ed. 34), 30100 Murcia, Spain*
[2]*Dpto. Física Aplicada, Universidad de Zaragoza, 50009 Zaragoza, Spain*
[3]*Dpto. Biología Celular, Histología y Farmacología, Facultad de Medicina, Universidad de Valladolid, 47005 Valladolid, Spain*
[*]*bueno@um.es*

Abstract: The organization of the corneal stoma is modified due to different factors, including pathology, surgery or external damage. Here the changes in the organization of the corneal collagen fibers during natural healing after chemical burn are investigated using second harmonic generation (SHG) imaging. Moreover, the structure tensor (ST) was used as an objective tool for morphological analyses at different time points after burn (up to 6 months). Unlike control corneas that showed a regular distribution, the collagen pattern at 1 month of burn presented a non-organized arrangement. SHG signal levels noticeably decreased and individual fibers were hardly visible. Over time, the healing process led to a progressive re-organization of the fibers that could be quantified through the ST. At 6 months, the stroma distribution reached values similar to those of control eyes and a dominant direction of the fibers re-appeared. The present results show that SHG microscopy imaging combined with the ST method is able to objectively monitor the temporal regeneration of the corneal organization after chemical burn. Future implementations of this approach into clinically adapted devices would help to diagnose and quantify corneal changes, not only due to chemical damages, but also as a result of disease or surgical procedures.

1. Introduction

The cornea is the frontal outer component of the eye and has two important functions: ocular refraction (2/3 of the total) and protection of the inner ocular structures [1]. Nearly 90% of the cornea is constituted by the stroma, a layer mainly composed of collagen and proteoglycans (such as lumican, keratocan and decorin). These proteoglycans play an important role in collagen fibrillogenesis, matrix assembly, hydration and thus in extracellular matrix (ECM) organization [2]. This ECM is responsible for corneal transparency because of the particular organizations of the collagen fibrils within the stroma.

Due to its location, the cornea might be exposed to different damages and non-controlled changes as a result of surgery, physical trauma or chemical burns among others. Chemical injuries are usually caused by acid and alkali agents and represent 11.5–22.1% of ocular traumas [5]. They take place accidentally in the workplace, commonly in industrial and chemical laboratories (30–50 year old people), and at home (children aged 1–2 years have a significant risk). Alkali injuries are more frequent than acidic injuries. Alkali agents penetrate into the corneal stroma producing the liquefaction of proteoglycans and collagen, as well as destroying cells. This leads to a significant loss of corneal transparency and sometimes permanent blindness [4].

#412819 https://doi.org/10.1364/BOE.412819
Journal © 2021 Received 16 Oct 2020; accepted 22 Dec 2020; published 11 Jan 2021

Biomedical Optics EXPRESS

Corneal chemical injuries require emergency action and immediate evaluation [3]. Aggressive treatments to achieve the best result or avoid the worst outcome are imperative [4]. Wounds produced by alkali burns are some of the most difficult to treat. Prognosis of evolution depends on the damage suffered by the corneal and conjunctival epithelium, the degree of limbal blanching, and area and density of the corneal opacification [6]. The wound healing process after alkali burn presents several complications such as slow reepithelization, persistent ulcerations, neovascularization and severe opacification [7]. This extended ulceration promotes the deposition of excessive ECM in the wound surface that, sometimes, results in scar formation.

Long-term studies on corneal tissue recovery after alkali burns are scarce in the literature. Using laser scanning confocal microscopy, Xiang and co-workers reported full corneal epithelium recovery three months after burn (in corneas presenting a very severe damage) [8]. Other authors have employed OCT imaging to visualize changes in corneal transparency due to burns produced by topical application of corrosive solutions. They found an increase in light scattering within the stroma in ex-vivo corneas [9]. A recent study has demonstrated the dynamic and location of the different types of collagen and proteoglycans along the alkali wound healing [10].

Second harmonic generation (SHG) microscopy is a well-extended multiphoton imaging technique providing high-resolution visualization of non-stained collagen based tissues [11,12]. The corneal stroma is the paradigmatic example of biological tissue imaged by means of SHG microscopy where collagen fibers can be clearly visualized [13]. Although the spatial distribution of collagen fibers in control corneas has been extensively reported [14–16], the interest in the analysis and classification (both qualitative and quantitative) of non-healthy samples has increased considerably. These studies have explored and identify stromal changes due to pathologies [17–20], intraocular pressure [21] or surgery [22–25].

External damages and physical trauma in the cornea have also been explored with SHG microscopy [26–28]. Thermal burn injuries have been reported to show a significant reduction in SHG signal as a consequence of collagen denaturation and disorganization. SHG images of penetrating corneal scar tissue showed that the collagen pattern was irregularly arranged at the wound. In addition, outside of the wound, the collagen fibers tended to align parallel to the wound edges [29].

Alkali injures produce disruption of normal organization of the corneal stroma and a decrease in transparency. Moreover, wound healing processes involve cellular proliferation and migration, as well as collagen remodelling to restore corneal transparency [30]. However, to the best of our knowledge, quantitative studies dealing with the modifications in the stromal arrangement after alkali injuries have not been reported. Here, we propose a long-term investigation on the re-organization and natural healing process of the corneal stroma after alkali burn using SHG microscopy.

2. Methods

2.1. Experimental system

A research multiphoton microscope was used for SHG imaging of the corneas involved in the experiment. Details on this home-made instrument have been extensively reported elsewhere [16]. In brief, a Ti:sapphire femtosecond laser (800 nm wavelength and 76 MHz repetition rate) illuminates the sample. A couple of non-resonant galvanometric mirrors allows XY scanning and a stepper motor coupled to the microscope objective (NA=0.5, 20x, dry long working-distance) is used for axial positioning within the sample under analysis. In the outgoing pathway, the signal travels back through the objective and a dichroic mirror (that splits this generated nonlinear signal from the incident light), and passes a narrow-band spectral filter placed in front of the detector. This filter ensures that only SHG signal reaches the detection unit. Image acquisition was controlled with home-made LabView™ software. A custom Matlab™ script was used for image processing.

Biomedical Optics EXPRESS

2.2. Animal model and tissue preparation

New Zealand albino adults rabbits (N=12) were used in this experiment. Animals were provided by "Granja San Francisco" (Navarra, Spain), a Spanish official provider of lab animals. The animals were anesthetized with ketamine hydrochloride (30 mg/kg; Ketolar, Parke Davis SA, Barcelona, Spain), xylazine (5 mg/kg; Rompun, Bayern, Leverkusen, Germany) followed by topical application of 0.5% tetracaine hydrochloride and 1 mg of oxybuprocaine (Colircusi Anestésico Doble, Alconcusí SA, Barcelona, Spain). Under anaesthesia, alkali burn was performed on the corneal apex of the left eye of the animals as detailed in [31]. The fellow eye of each animal was used as control. Corneal burns were induced by placing a filter paper soaked in 0.5N NaOH solution for 60 seconds. After this time, the filter paper was removed, and the eye washed with sterile phosphate-buffered saline solution (PBS).

The animals were euthanized by an intracardiac injection of sodic pentobarbital after 1 (N=3), 3 (N=3), 5 (N=3) and 6 months of burn (N=3). For each group the animals were randomly chosen. Then, the ocular globes were enucleated and the corneas excised, fixed in 4% buffered paraformaldehyde for 24 h and rinsed in buffer phosphate (0.1 M). Further details on this part of the procedure can be found in [32].

The herein experiment was approved by the Animal Research and Welfare Ethics Committee of the Universities of Valladolid and Murcia. Animal care followed the guidelines of the Association for Research in Vision and Ophthalmology (ARVO) Statement for the Use of Animals in Ophthalmic and Vision Research.

2.3. Imaging and analysis procedures

Each non-stained cornea was placed on a glass bottom dish (170-µm thickness) filled with buffer phosphate and placed on the microscope stage for SHG imaging. Series of 3 individual frames of the corneal stroma (at the apex location) were recorded every 20 µm depth (total imaged depth: 140 µm). A frame rate of 1 Hz for a field-of-view of 180×180 µm^2 was used. In order to reduce noise and enhance contrast, every final SHG image was the average of those individual frames. The first location within the stroma where the SHG signal appeared (Bowman's layer) was established as the zero-reference (i.e. 0-µm depth position) [16].

As an illustrative example, Fig. 1 shows an *in vivo* cornea (one month after burn, Fig. 1(a)) and a specimen ready to be imaged with the SHG microscope (Fig. 1(b)). The opacification produced by the alkali burn is clearly visible in both pictures.

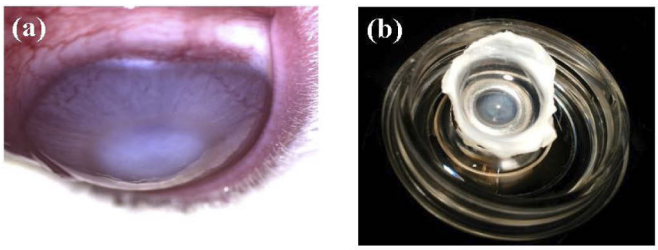

Fig. 1. Burned cornea in living (a) and excised (b) experimental conditions.

To explore the structural organization of the collagen fibers of each SHG image, the structure tensor (ST) method was applied. A detailed description of the ST formalism can be found in [33]. Briefly, the ST is a mathematical tool that provides quantitative information on the preferential orientation (PO) of the fibers through the calculation of three parameters known as the degree of isotropy (DoI), the histogram of PO, and the structural dispersion (SD). This latter is defined as the standard deviation of the PO histogram.

Biomedical Optics EXPRESS

The DoI ranges between 0 (non-organized structure and absence of PO) and 1 (parallel-arranged structure and well-defined PO). A partially organized collagen distribution verifies the condition $0.2 \leq DoI < 0.7$ [33]. The histogram shows the relative frequency of PO throughout the entire image. If a PO exists, the distribution can be fitted by a Gaussian curve centred on the corresponding PO value. SD will be larger than 40° if a non-organized arrangement is present. When $SD \leq 20°$, the image contains fibers arranged in a quasi-aligned manner. Values in between correspond to a partially organized distribution. A linear correlation between DoI and SD has been reported, thus only one of both parameters is required to describe the spatially resolved distribution of collagen fibers.

3. Results

Figure 2 presents the SHG intensity profiles as a function of depth for a control (red line) and a 1-month after burn (blue line) corneas. Data have been normalized for a direct comparison. For both experimental conditions, the recorded SHG signal decreases with depth. However, the reduction in the chemical damaged sample is more pronounced due to the presence of corneal edema (as a result of the alkali burn). For example, at 50-μm depth, whereas the signal decreases 20% in the control cornea, this goes up to 70% in the burned one. These differences were found to be statistically different ($p < 0.0001$).

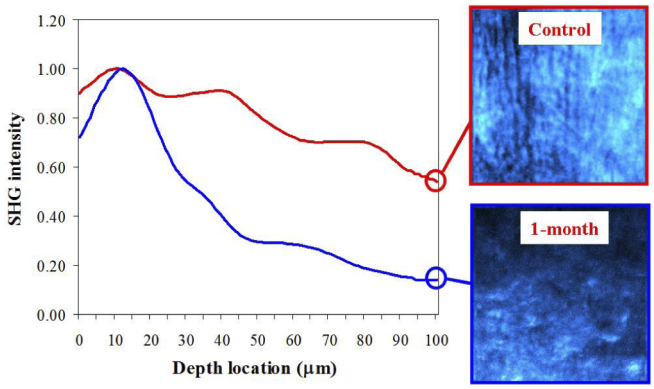

Fig. 2. Normalized SHG intensity depth profiles for a control (red) and a burned (blue) cornea. The right panels show representative SHG images at a depth location of 100 μm. For a better comparison the images are shown with the same colour scale. Image size: 180×180 μm^2.

This drastic attenuation in signal leads to a reduced SHG performance at deeper locations, what can be better understood comparing the images on the right panels. These represent SHG images for a depth location of 100 μm for both specimens. In the control cornea the collagen fibers are readily visible (mainly arranged in a vertical direction for this particular image). On the opposite, in the damaged sample the SHG signal is much lower (more than one half) and the fibers are not visible at all. For deeper locations, burned corneas provided SHG images of very low signal, poor quality and difficult to be processed. Due to this, along this paper we have centred our study in the SHG images of the anterior corneal stroma (from 0 to 100 μm depth), where the images are of enough quality to be analyzed and compared.

Figure 3 depicts a set of representative corneal SHG images at different time points after alkali burn (i.e. stages of natural wound healing). Figure 3(a) corresponds to a control sample that can be used for direct comparisons. This image shows the normal collagen arrangement in a healthy rabbit corneal stroma: a regular spatial distribution of the fibers oriented along a well-defined PO. This organized collagen pattern drastically changes after chemical injury. In

Biomedical Optics EXPRESS

particular, the stroma of a sample after one month of burn can be observed in Fig. 3(b). Unlike the control cornea, a non-organized pattern is present here, with an apparent absence of PO. At 3 months, wound recovery and some collagen re-organization start to be visible (not shown). After 5 months (Fig. 3(c)) the healing process begins to remodel the collagen distribution and more dense and packed collagen structure appears. Finally, at 6 months of burn, the stroma shows a partially regenerated pattern (Fig. 3(d)), with fibers along a PO, although not as noticeable as that found in the control sample (probably due to an incomplete corneal natural healing process).

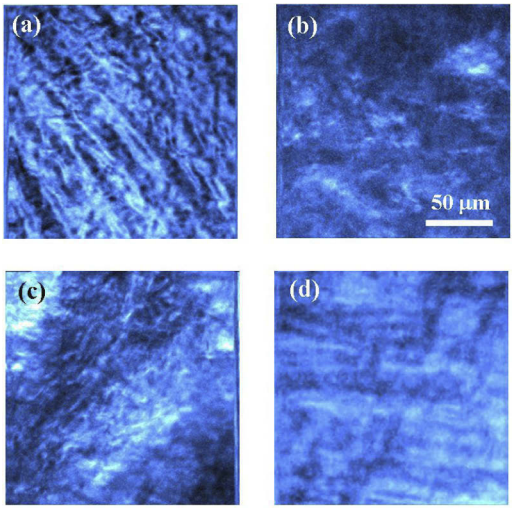

Fig. 3. Representative SHG images of the rabbit cornea as a function of the time after chemical burn. Control (a); after 1 (b), 5 (c) and 6 months (d) of burn. All images correspond to the anterior stroma.

A simple visualization of the SHG images provides qualitative information. However, sometimes is difficult to analyze or comment on the changes suffered by the corneal structure. Thus, for a better description and understanding of the denaturation/healing effects of the stromal collagen due to chemical burn, a quantitative study must be carried out.

In that sense, the DoI maps corresponding to samples of Fig. 3 are shown in Fig. 4. The insets are the DoI values averaged across the entire map.

As expected, the DoI map for the control sample is much lighter than that of the cornea after 1 month of burn. That is, the control sample is characterized by a high DoI value, which corresponds to a quasi-organized collagen structure (DoI>0.70, Fig. 4(a)) [33]. This natural arrangement of the collagen turns into a non-organized structure under alkali burn (with a DoI lower than 0.20, Fig. 4(b)). As healing time increases, the DoI maps become lighter revealing a progressive recovery in terms of collagen organization (Fig. 4(c) and Fig. 4(d)). Similar maps were found for all the damaged corneas involved in the experiment.

Figure 5 presents the histograms of PO corresponding to the maps presented in Fig. 4. As expected, for the control cornea, a fairly well-organized structure (low SD, 7°) with a remarkable PO at −50° is present. The 1-month after-burn cornea presents a PO histogram with a homogeneous distribution (i.e. absence of PO), that reveals a non-organized collagen distribution with a high SD (72°). At 5 months, the cornea has turned into a partially organized structure (SD=29°, PO~50°). This level of organization increases at 6 months of healing (SD=18°) with a visible PO (at approximately 0° for the sample here shown). This increase in fiber organization leads to both a decrease in SD and a reduction of the peak width (centred in PO).

Biomedical Optics EXPRESS

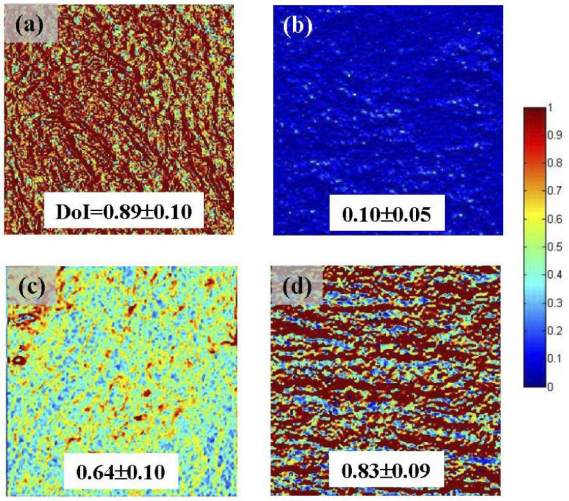

Fig. 4. DoI maps of the samples shown in the previous figure. The insets represent the averaged DoI value across each map. A simple visualization of the maps provides an idea about the general behaviour of the parameter as a function of time.

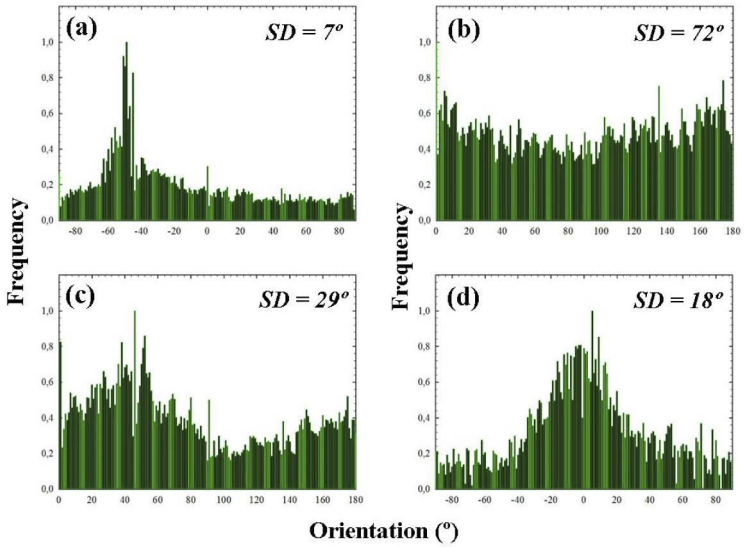

Fig. 5. Histograms of PO distribution computed by applying the ST to the corneal SHG images of Fig. 2. The corresponding SD values are also included for direct comparisons.

Figure 6 depicts the averaged DoI values as a function of the time after burn for all the corneas involved in the experiment. For each time point the bars represent the mean across all specimens and corneal layers. The data for the control samples have also been included. The differences among the different groups have been statistically analyzed.

As expected from the previous results, the plot shows a drastic fall in DoI values between the control group and the one after 1 month of burn damage. The statistical analysis revealed that this difference was significant ($p<0.0001$). Then, a progressive increase in DoI appears with time (i.e. higher organization), reaching DoI values similar to those found for the control samples

Biomedical Optics EXPRESS

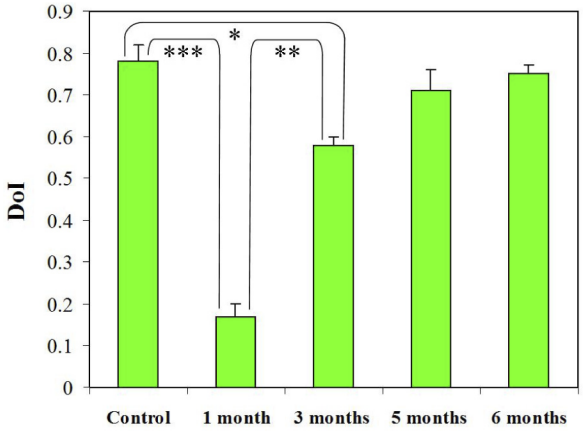

Fig. 6. Averaged DoI values as a function of the time after alkali burn (i.e. wound healing period). Data of each group correspond to the mean values for all specimens and depth locations (from 0 to 100 µm). Error bars indicate the standard deviation.

at 6 months. Differences between the groups 1- and 3-months after burn were also significant ($p<0.005$). In addition, the DoI values did not differed significantly when comparing control and 5- or 6-month after burn corneas. This implies that for those time points the natural wound healing has made the corneas mostly recover their regular stroma arrangement.

4. Discussion and conclusions

In this study, we have used SHG microscopy images and the ST algorithm to quantitatively analyze the natural wound healing process of the corneal collagen after alkali burn. The different numerical parameters provided by the ST have served as objective tools to analyze the temporal evolution (1, 3, 5 and 6 months) of the spatial arrangement of the collagen fibers of the stroma.

In control corneas, there is a SHG signal uniform decrease with depth. However, due to the edema and the ECM deposition produced by the wound healing process, a drastic SHG intensity attenuation occurred in burned specimens. Thus, measurements were limited to a depth of 100-µm within the anterior stroma.

The corneal collagen is largely affected one month after burn. It presents a high deposition of collagen fibers, as well as proteoglycans [10], and shows a non-organized pattern (SD>70°). Individual fibers are hardly visible at this time point, probably because the non-proper interaction between the collagen molecules and leucine-rich proteoglycans [34]. As expected, this is in noticeable contrast with control corneas (SD<20°) where a fairly regular arrangement was found, as well as the presence of a PO. At 3 months, some collagen re-organization associated with healing appears. Quantitatively, the DoI presents a statistically significant 3-fold increase. As time passes, this wound recovery is in progress and the collagen arrangement is gaining structural order, what can be objectively seen in the increase of DoI appearing at 5 months. This is closely linked to the reduction of edema and then, to the increase of corneal transparency [10]. For the final time point here checked (6 months after burn), collagen remodelling is still taking place. Although individual collagen fibers begin to be delineated, they are still thicker that those corresponding to control specimens. The value of SD, as seen in the corresponding PO histogram, indicates that the tissue regeneration associated with healing might not be complete yet.

Our results are coherent with previous SHG studies dealing with corneal changes as a result of different external damages. In particular, edematous corneas (produced by immersion in deionized water for 2 h) were shown to worsen the depth-dependent SHG signal decay and to

Biomedical Optics EXPRESS

present heterogeneous structural alterations [18]. The stroma was also found to be disorganized due to photo-thermal effects following laser irradiation [27]. Depending on the external strain, the cornea structure also showed marked differences [35]. As a result of temperature rising, the stroma was reported to undergo distinct structural stages [26]. These ranged from a decrease in SHG intensity from 30° to 45°C, and an organization in locally dense bundles (due to thermal disruption of cross-linking elements in the corneal stroma) at temperatures between 53° and 77°C, to the absence of organized histological structure and the lack of SHG signal at 90°C (when the non-centrosymmetric structure of collagen fibrils responsible for generating the SHG signal has been completely destroyed). Later, quantitative analyses of thermal transitions in the corneal stroma suggested three destructuration stages at different hierarchical levels of collagen assembly [36].

At this point, it is interesting to highlight a recent SHG microscopy quantitative study by these authors on edema temporal progression (generated by hyper-hydration). It was shown that the structural order of the collagen fibers decreases as the corneal edema increases [20]. Results here reported agree with that previous experiment. However, unlike the assessment and characterization of those increasing edematous processes, in the present work the analysis was done in the opposite direction (i.e. edema progressive reduction and cornea recovering). That is, the dramatic effect of the chemical burn (including edema, denaturation and disorganization) is slowly disappearing during healing: the more time after damage the higher the collagen fiber organization appearing.

To conclude, corneas exposed to alkali burn undergo a severe opacification due to an enormous synthesis of ECM, to recover from the denaturation produce by the alkali. The combination of SHG microscopy and the ST indicates that this effect is closely associated with a complete loss of collagen structural order. Within the period here analyzed collagen natural healing leads to a progressive increase in the organization level of the fibers. Stroma arrangement begins to gain organization at the time individual fibers appear again. Probably due to a non-complete wound healing, the collagen organization did not reach the level of a control sample at the final stage checked (i.e. 6 months). This suggests that for the herein animal model, this type of chemical damages could require longer recovering periods. These results confirm that the imaging tools here used are accurate and effective to track damages suffered by the corneal collagen in a quantitative manner.

Once SHG imaging has been reported to be safe in living human eyes [37], future implementations of our approach into clinical environments might help to objectively diagnose corneal damages and surgical-induced disorder states, to monitor corneal wound healing after pharmacological treatments or surgical outcomes, and to accurately establish recovery time periods.

Funding. Instituto de Salud Carlos III (PI15/01906); Fundación Séneca (19897/GERM/15).

Acknowledgments. The authors thank D. Párraga, OD, MSc, for her help during different steps of this work and Cristina Herrero-Pérez for technical assistance.

Disclosures. The authors declare no conflicts of interest and have no proprietary interest in any of the materials mentioned in this article.

References

1. K. M. Meek, "The cornea and sclera,", in *Collagen*, P. Fratzl, ed. (Springer, 2008), pp. 359–396.
2. D. Massoudi, F. Malecaze, and S. D. Galiacy, "Collagens and proteoglycans of the cornea: importance in transparency and visual disorders," Cell Tissue Res. **363**(2), 337–349 (2016).
3. W. J. Scott, N. Schrage, and C. Dholman, "Emergency eye rinse for chemical injuries: New considerations," JAMA Ophthalmol. **133**(3), 245 (2015).
4. P. Singh, M. Tyagi, Y. Kumar, K. K. Gupta, and P. D. Sharma, "Ocular chemical injuries and their management," Oman J. Ophthalmol. **6**(2), 83–86 (2013).
5. N. Sharma, M. Kaur, T. Agarwal, V. S. Sangwan, and R. B. Vajpayee, "Treatment of acute ocular chemical burns," Surv. Ophthalmol. **63**(2), 214–235 (2018).

Biomedical Optics EXPRESS

6. L. Chen, J. Zhong, S. Li, W. Li, B. Wang, Y. Deng, and J. Yuan, "The long-term effect of tacrolimus on alkali burn-induced corneal neovascularization and inflammation surpasses that of anti-vascular endothelial growth factor," Drug Des., Dev. Ther. **12**, 2959–2969 (2018).
7. Q. Yi and W. J. Zou, "The wound healing effect of Doxycycline after corneal alkali burn in rats," J. Ophthalmol. **2019**, 1–10 (2019).
8. J. Xiang, Q. Le, Y. Li, and J. Xu, "In vivo confocal microscopy of early corneal epithelial recovery in patients with chemical injury," Eye **29**(12), 1570–1578 (2015).
9. F. Spöler, M. Först, and H. Kurz, "Dynamic analysis of chemical eye burns using high-resolution optical coherence tomography," J. Biomed. Opt. **12**(4), 041203 (2007).
10. E. Lorenzo-Martín, P. Gallego-Muñoz, S. Mar, I. Fernández, P. Cidad, and M. C. Martínez-García, "Dynamic changes of the extracellular matrix during corneal wound healing," Exp. Eye Res. **186**, 107704 (2019).
11. P. J. Campagnola, H. A. Clark, W. A. Mohler, A. Lewis, and L. M. Loew, "Second-harmonic imaging microscopy of living cells," J. Biomed. Opt. **6**(3), 277–286 (2001).
12. J. M. Bueno, F. J. Ávila, and Pablo Artal, "Second harmonic generation microscopy: a tool for quantitative analysis of tissues," in *Microscopy and Analysis*, S. G. Stanciu, ed. (IntechOpen, 2016).
13. A. T. Yeh, N. Nassif, A. Zoumi, and B. J. Tromberg, "Selective corneal imaging using combined second-harmonic generation and two-photon excited fluorescence," Opt. Lett. **27**(23), 2082–2084 (2002).
14. N. Morishige, W. M. Petroll, T. Nishida, M. C. Kenney, and J. V. Jester, "Noninvasive corneal stromal collagen imaging using two-photon-generated second-harmonic signals," J. Cataract Refractive Surg. **32**(11), 1784–1791 (2006).
15. F. Aptel, N. Olivier, A. Deniset-Besseau, J.-M. Legeais, K. Plamann, M.-C. Schanne-Klein, and E. Beaurepaire, "Multimodal Nonlinear Imaging of the Human Cornea," Invest. Ophthalmol. Visual Sci. **51**(5), 2459–2465 (2010).
16. J. M. Bueno, E. J. Gualda, and P. Artal, "Analysis of corneal stroma organization with wavefront optimized nonlinear microscopy," Cornea **30**(6), 692–701 (2011).
17. H. Y. Tan, Y. Sun, W. Lo, S. J. Lin, C. H. Hsiao, Y. F. Chen, S. C. Huang, W. C. Lin, S. H. Jee, H. S. Yu, and C. Y. Dong, "Multiphoton fluorescence and second harmonic generation imaging of the structural alterations keratoconus ex vivo," Invest. Ophthalmol. Visual Sci. **47**(12), 5251–5259 (2006).
18. C. M. Hsueh, W. Lo, W. L. Chen, V. A. Hovhannisyan, G. Y. Liu, S. S. Wang, H. Y. Tan, and C. Y. Dong, "Structural characterization of edematous corneas by forward and backward second harmonic generation imaging," Biophys. J. **97**(4), 1198–1205 (2009).
19. A. Batista, H. G. Breunig, A. König, A. Schindele, T. Hager, B. Seitz, and K. König, "High-resolution, label-free two-photon imaging of diseased human corneas," J. Biomed. Opt. **23**(03), 1 (2018).
20. F. J. Ávila, P. Artal, and J. M. Bueno, "Quantitative discrimination of healthy and diseased corneas with second harmonic generation microscopy," Trans. Vis. Sci. Tech. **8**(3), 51 (2019).
21. Q. Wu and A. T. Yeh, "Rabbit cornea microstructure response to changes in intraocular pressure visualized by using nonlinear optical microscopy," Cornea **27**(2), 202–208 (2008).
22. H. Y. Tan, Y. L. Chang, W. Lo, C. M. Hsueh, W. L. Chen, A. A. Ghazaryan, P. S. Hu, T. H. Young, S. J. Chen, and C. Y. Dong, "Characterizing the morphologic changes in collagen crosslinked–treated corneas by Fourier transform–second harmonic generation imaging," J. Cataract Refractive Surg. **39**(5), 779–788 (2013).
23. J. M. Bueno, E. J. Gualda, A. Giakoumaki, P. Pérez-Merino, S. Marcos, and P. Artal, "Multiphoton microscopy of ex vivo corneas after collagen cross-linking," Invest. Ophthalmol. Visual Sci. **52**(8), 5325–5331 (2011).
24. E. J. Gualda, J. R. Vázquez de Aldana, M. C. Martínez-García, P. Moreno, J. Hernández-Toro, L. Roso, P. Artal, and J. M. Bueno, "Femtosecond infrared intrastromal ablation and backscattering-mode adaptive-optics multiphoton microscopy in chicken corneas," Biomed. Opt. Express **2**(11), 2950–2960 (2011).
25. J. M. Bueno, R. Palacios, A. Pennos, and P. Artal, "Second-harmonic generation microscopy of photocurable polymer intrastromal implants in ex-vivo corneas," Biomed. Opt. Express **6**(6), 2211–2219 (2015).
26. H.-Y. Tan, S. W. Teng, W. Lo, W. C. Lin, S. J. Lin, S. H. Jee, and C. Y. Dong, "Characterizing the thermally induced structural changes to intact porcine eye, Part 1: Second harmonic generation imaging of cornea stroma," J. Biomed. Opt. **10**(5), 054019 (2005).
27. P. Matteini, F. Ratto, F. Rossi, R. Cicchi, C. Stringari, D. Kapsokalyvas, F. S. Pavone, and R. Pini, "Photothermally-induced disordered patterns of corneal collagen revealed by SHG imaging," Opt. Express **17**(6), 4868–4878 (2009).
28. W. Lo, Y. L. Chang, J. S. Liu, C. M. Hseuh, V. Hovhannisyan, S. J. Chen, H. Y. Tan, and C. Y. Dong, "Multimodal, multiphoton microscopy and image correlation analysis for characterizing corneal thermal damage," J. Biomed. Opt. **14**(5), 054003 (2009).
29. S. Teng, H. Tan, Y. Sun, S. J. Lin, W. Lo, C. M. Hsueh, C. H. Hsiao, W. C. Lin, S. C. Huang, and C. Y. Dong, "Multiphoton fluorescence and second-harmonic-generation microscopy for imaging structural alterations in corneal scar tissue in penetrating full-thickness wound," Arch. Ophthalmol. **125**(7), 977–978 (2007).
30. M. E. Fini and B. M. Stramer, "How the cornea heals: cornea-specific repair mechanisms affecting surgical outcomes," Cornea **24**(Supplement 1), S2–S11 (2005).
31. P. Gallego-Muñoz, E. Lorenzo-Martín, I. Fernandez, C. Herrero-Perez, and M. C. Martínez-García, "Nidogen-2: location and expression during corneal wound healing," Exp. Eye Res. **178**, 1–9 (2019).

Biomedical Optics EXPRESS

32. J. M. Bueno, F. J. Ávila, and M. C. Martínez-García, "Quantitative analysis of the corneal collagen distribution after in vivo cross-linking with second harmonic microscopy," BioMed Res. Int. **2019**, 1–12 (2019).
33. F. J. Ávila and J. M. Bueno, "Analysis and quantification of collagen organization with the structure tensor in second harmonic microscopy images of ocular tissues," Appl. Opt. **54**(33), 9848–9854 (2015).
34. J. R. Hassell and D. E. Birk, "The molecular basis of corneal transparency," Exp. Eye Res. **91**(3), 326–335 (2010).
35. Q. Wu, B. E. Applegate, and A. T. Yeh, "Cornea microstructure and mechanical responses measured with nonlinear optical and optical coherence microscopy using sub-10-fs pulses," Biomed. Opt. Express **2**(5), 1135–1146 (2011).
36. P. Matteini, R. Cicchi, F. Ratto, D. Kapsokalyvas, F. Rossi, M. de Angelis, F. S. Pavone, and R. Pini, "Thermal transitions of fibrillar collagen unveiled by second-harmonic generation microscopy of corneal stroma," Biophys. J. **103**(6), 1179–1187 (2012).
37. F. J. Ávila, A. Gambín, P. Artal, and J. M. Bueno, "In vivo two-photon microscopy of the human eye," Sci. Rep. **9**, 10121 (2019).